University of Baghdad
College of Engineering
JOURNAL OF ENGINEERING

Journal of Engineering
journal homepage: www.jcoeng.edu.iq
Volume 32 Number 9 September 2026

Experimental Investigation of Hydraulic Jump Control in Rectangular Channels using Movable Thin-Crested Sills

Rizgar Ahmed Karim*, **Bahram Abdalrahman Faraj**

Department of Water Resources Engineering, College of Engineering, University of Sulaimani, Sulaimani, Iraq

ABSTRACT

Hydraulic jumps are a fundamental phenomenon in open channel hydraulics, playing a critical role in energy dissipation and stilling basin design. Experimental research was conducted to investigate the hydraulic jump controlled with a thin-crested sill of varying heights and positions, which has not been previously investigated. Therefore, this experimental study was conducted to investigate hydraulic jump control using a thin-crested sill of varying heights and positions. The exact location of the hydraulic jump within the horizontal open channel should be known to prevent any damage to the surrounding structures. In total, 130 experiments were performed with initial Froude numbers ranging from 3.42 to 8.93. Measurements included the basic variables, such as initial and sequential depths, jump lengths, energy losses for sluice gate openings, and different discharge rates. Findings indicate that although the sill placement had minimal effect on the sequent depth ratio, it had a significant reduction in jump length, jump position, and energy dissipation in the stilling basin. The experimental sequent depth ratio (y_2/y_1) showed close agreement with the values predicted by Bélanger's equation. In addition, regression models developed to estimate the sequent depth ratio, jump length, energy loss, and optimal sill location achieved coefficients of determination ranging from 0.82 to 0.98. These results provide practical design guidance for selecting appropriate sill dimensions and locations to ensure complete hydraulic jump formation and effective energy dissipation in stilling basins.

Keywords: Movable thin-crested sill, Control of hydraulic jump, Sill height, Sill position, Stilling basin.

1. INTRODUCTION

Hydraulic jump, a common occurrence within channel flows, has been extensively studied in hydraulic engineering. A hydraulic jump is generated when supercritical flow changes to subcritical flow, resulting in substantial energy dissipation and intense turbulent mixing. Its behavior, including the location and stability of the jump, is influenced by several hydraulic parameters, such as the discharge, Froude number, tailwater depth, sluice-gate opening, and

*Corresponding author
Peer review under the responsibility of University of Baghdad.
https://doi.org/10.31026/j.eng.2026.09.02

Article received: 12/04/2026
Article revised: 26/07/2026
Article accepted: 28/07/2026
Article published: 01/09/2026

the configuration of downstream control structures. These jumps take place when a rapid transition from low to high flow depth occurs, leading to a sudden rise in water depth **(Gupta and Mehta, 2010; Akan and Iyer, 2021)**. **(Forster and Skrinde, 1950)** study on forced hydraulic jumps by means of a continuous sill was the first basic study on this approach **(Pagliara and Peruginelli, 2000; Chow, 1959)**. They emphasized control and prevention of erosion on the riverbed outside the stilling basin, under free downstream flow conditions **(Mahmoud and Mohamed, 2022; Bachir et al., 2022)**. The installation of a sill changes the downstream water level and pressure distribution, thereby affecting the sequent depth, turbulence characteristics, and the amount of energy dissipated. Consequently, both the sill height and its position are key factors in controlling hydraulic jump stability and overall stilling basin performance. Various sill types, including board-crested weirs, sharp-crested weirs, and sudden falls and rises, can induce or form hydraulic jumps. Their functions are to ensure jump formation and to control its position across all expected flow conditions **(Dardeer, 2022; Erryanto and Dermawan, 2024)**. Accessories such as sills and baffle blocks are also used in creating the kind of forced or unforced hydraulic jump. Sills that are properly designed may alter the jump's location and formation **(Abbaszadeh et al., 2023; Omid et al., 2010)**. Positions of the jump also depend on factors like discharge, channel geometry, and the location of the sill **(Mundo-Molina and Díaz Pérez, 2019; Yıldız et al., 2020)**. The hydraulic jump length and energy variations have been quantified to enhance energy dissipation and avoid damage **(Mahmoud and Mohamed, 2022; Li, 1995).** Although the research on fixed weirs is widespread, the research on movable weirs is less common **(Kim et al., 2015).** The researchers came up with experimental work on the use of a sill in the control of jumps **(Bachir et al., 2022; Daneshfaraz et al., 2023)**. Instead, the others used broad-crested types in a rectangular channel to do the same **(Ghordnooshahre et al., 2010; Achour and Amara, 2023)**. Some also applied a sudden rise at the base of a square open channel to provide the same effect **(Dixit et al., 2016; Jadhav and Karkhanis, 2016)**. **(Hager and Li, 1992; Jamshidi et al., 2025)** investigated a sill-controlled energy dissipater. They evaluated the impact of a continuous, transverse sill on the hydraulic jump of a rectangular channel with two- and three-dimensional flows. Even though experimental and numerical analysis have demonstrated that the sill's thickness has no discernible impact on the dissipation mechanism and flow behavior **(Hager, 2013; Movahed et al., 2018)**, some researchers used the broad-crested and the thin-crested sills in a rectangle channel **(Omid et al., 2010)**, U-shaped channel **(Achour and Debabeche, 2003)**, and horizontal symmetric triangular channel to control the hydraulic jumps **(Debabeche and Achour, 2007; Samadi-Boroujeni et al., 2013)**. Experiments are carried out to evaluate the impact of a vertical continuous single sill and its position on controlling the length and depth of a hydraulic jump **(Alikhani et al., 2010; Fathi-Moghadam et al., 2011)**. To design stilling basins, a numerical model and an equation were developed to model hydraulic jumps in rectangular channels **(Eltoukhy, 2016; Nandi et al., 2020)**.

This paper describes an experimental study on how to control hydraulic jumps with a movable thin-crested sill. The study examines a wide range of sill heights and their corresponding positions with respect to the hydraulic jump. This comprehensive testing allows the results to be extended to some flow states. The main aim is to find the best sill height and position that will ensure that the hydraulic jump is in a complete formation in the stilling basin.

2. MATERIALS AND METHOD

The hydraulic laboratory at the University of Sulaimani's Department of Water Resources Engineering hosted the experiment. It utilized the S6-MKII tilting flume, featuring glass sides and a stainless-steel bed. This flume has a 300 mm wide by 450 mm deep working section and a standard 7.5 m length. Perspex side walls allow clear observation of hydraulic jump positions, while rails atop these walls support sliding point gauges for depth measurements along the channel **(Karim and Mohammed, 2020)**
The longitudinal section of the experimental flume and the hydraulic characteristics of the hydraulic jump under the influence of a sharp-crested sill are shown in **Fig. 1.** The experimental setup schematic diagram is displayed in **Fig. 2**.

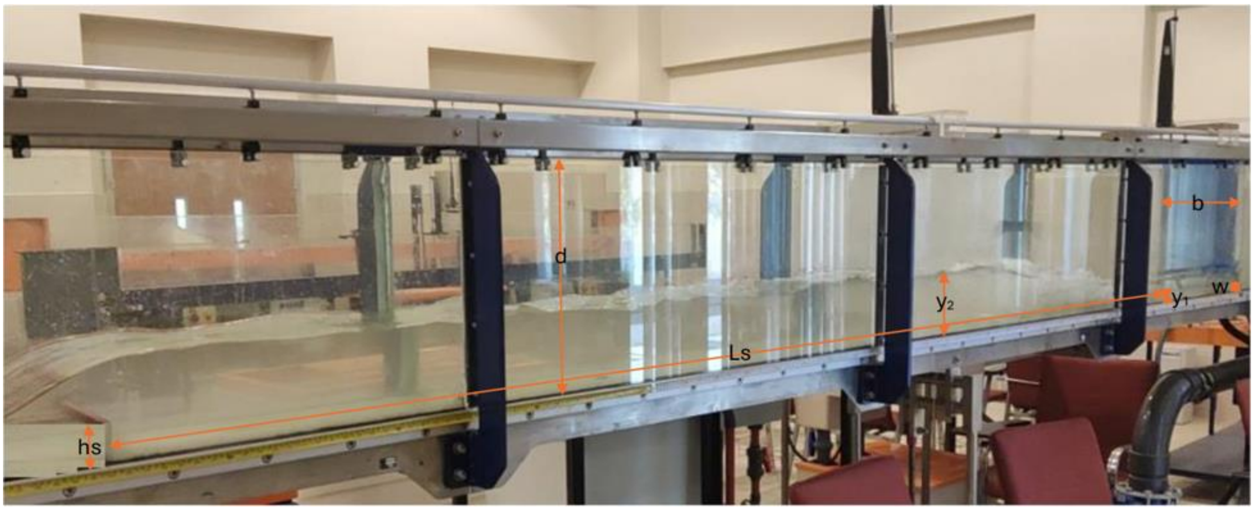

Figure 1. Illustrates the longitudinal section of the experimental flume and the hydraulic characteristics of the hydraulic jump controlled by a sharp-crested sill.

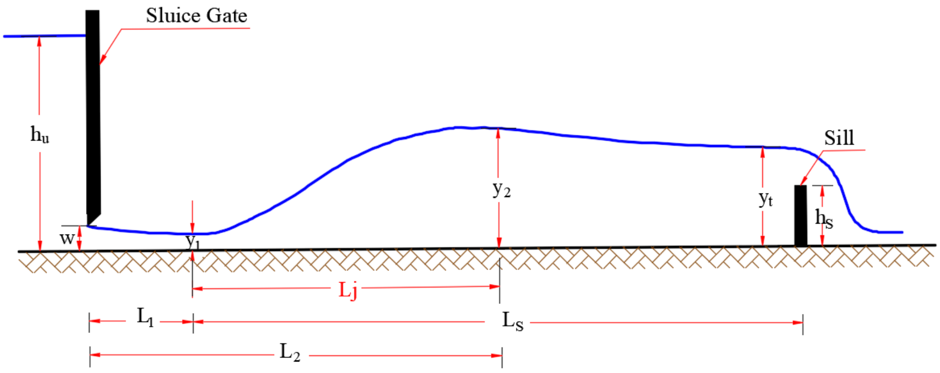

Figure 2. Schematic layout of the experimental model

Previous research has indicated that a thin-crested sill can effectively control a hydraulic jump. Accordingly, movable sills with heights of 2, 4, 5, 6, and 8 cm were installed to raise the downstream water level and promote hydraulic jump formation within the stilling basin. The sills were fabricated from Perspex glass and extended across the entire width of the experimental flume. Each sill featured a thin crest, while a 2.5 mm groove was provided along its sides. A plastic tube of the same diameter was fitted into the groove to facilitate smooth sill movement and minimize water leakage along the sides. Experiments involved

conducting multiple runs at varying discharge rates. A hydraulic jump was generated using a sluice gate (440 mm high, 10 mm thick, featuring a streamlined lip). For each run, measurements were taken of the initial depth (y_1), sequent depth (y_2), and the lengths L_1, L_2, and Ls. This procedure was repeated sequentially for sluice gate openings (w) of 10, 15, 20, 30, 40, and 50 mm to create free hydraulic jumps. A rail-mounted point gauge with an accuracy of 0.1 mm was used to measure the flow depth. Lengths were determined using a measuring tape (1 mm accuracy) fixed along a rail. Discharge was measured using an electromagnetic flowmeter (±0.1 L/s accuracy) **(Al-Suhili et al., 2023)**
The experiments, shown in **Table 1**, were initiated using the smallest gate opening, the lowest sill height, and the sill position closest to the gate. The channel was supplied with the minimum discharge required to form a hydraulic jump near the gate. After steady-flow conditions were achieved, flow discharge, sill position, and flow depths were measured at the centerline of the flume to avoid sidewall effects. As the discharge increased, the sill was gradually moved downstream to maintain the free hydraulic jump close to the gate and prevent downstream submergence of the gate.

Table 1. Recorded data of some of the runs in the laboratory

Q (L/sec)	hu (cm)	w (cm)	y_1 (cm)	y_2 (cm)	L_1 (cm)	L_2 (cm)	hs (cm)	Ls (m)
3.16	15.50	1.00	0.71	5.12	25.00	52.00	2.00	1.75
6.44	29.50	1.50	0.98	8.45	55.00	155.00	4.00	2.70
10.60	44.60	2.00	1.17	11.98	95.00	180.00	5.20	4.87
12.95	26.20	3.00	1.88	11.63	97.00	170.00	4.00	2.53
15.60	37.00	3.00	1.83	14.32	75.00	166.00	6.00	3.80
19.90	37.80	4.00	2.41	16.30	78.00	188.00	6.00	4.22
22.35	30.00	5.00	3.60	15.90	86.00	165.00	5.20	4.97

Measurements were recorded after each adjustment. This procedure continued until the maximum discharge (30 L/s) and the furthest sill position (5 m) were reached. The gate opening was then increased, and the same sequence was repeated for each sill height until all experimental conditions had been tested.
For this research, 130 experiments were carried out with Froude numbers (Fr_1) varying between 3.42 and 8.93. Froude number is the ratio of inertial forces to gravitational forces, which is a measure of the impact of the gravity on the fluid flow. In the case of rectangular cross-sectional and horizontal channels **(Chow, 1959)**, the governing equations are represented by:

$$Fr = \frac{v}{\sqrt{gD}} \tag{1}$$

$$D = \frac{T}{A} \tag{2}$$

Where D is the hydraulic mean depth, g is the gravitational acceleration and T is the width of the free surface. Whereas in the case of rectangular channel **(Chaudhry, 2008)**, the expression can be written as:

$$Fr = \frac{v}{\sqrt{gy}} \tag{3}$$

With y denoting the flow depth.

The research does not adopt modelling (similitude). The objective of the research is to develop regression equations for the hydraulic jump length and location under different controlled hydraulic conditions, using experimental work data. These data are compared to theoretical equations using the same experimental flume dimensions and flows; hence, no geometrical similarity is required. The dynamic similarity is adopted through the use of the Froude number, as it is involving gravity force which is the main flow driving force for open channels.

The uncertainty analysis of the calculated hydraulic parameters was estimated using the root-sum-square (RSS) method, assuming that the measurement errors of the independent variables were random and uncorrelated. For a dependent variable [$R = f(x_1, x_2, \ldots, x_n)$], the combined uncertainty was determined as:

$$U_R = \sqrt{\left(\frac{\partial R}{\partial x_1} U_{X1}\right)^2 + \left(\frac{\partial R}{\partial x_2} U_{X2}\right)^2 + \ldots + \left(\frac{\partial R}{\partial x_n} U_{Xn}\right)^2} \tag{4}$$

Where U_R is the combined uncertainty of the calculated parameter, U_{xi} is the uncertainty associated with each measured variable, and $\partial R/\partial x_i$ represents the sensitivity coefficient of R with respect to x_i. The uncertainties of the measured variables were determined from the accuracies of the experimental instruments, including the point gauge and flow measuring devices. This procedure provides an estimate of the propagation of measurement errors into the derived hydraulic parameters **(Taylor, 1997).**

Since one of the main parameters is the sequent depth ratio, $R = \frac{y_2}{y_1}$, the propagated uncertainty becomes:

$$U_{y_2/y_1} = \sqrt{\left(\frac{1}{y_1} U_{y2}\right)^2 + \left(\frac{y_2}{y_1^2} U_{y1}\right)^2} \tag{5}$$

Likewise, for the Froude number,

$$U_{Fr} = \sqrt{\left(\frac{\partial Fr}{\partial V} U_V\right)^2 + \left(\frac{\partial Fr}{\partial y} U_y\right)^2} \tag{6}$$

The Nash–Sutcliffe Efficiency (NSE) was introduced as a model performance criterion for evaluating the agreement between observed and predicted hydraulic data and has since become one of the most widely used performance metrics in water resources modeling. Nash and Sutcliffe defined the model efficiency as:

$$\mathrm{NSE} = 1 - \frac{\sum_{i=1}^{n}(Q_{\mathrm{obs},i} - Q_{\mathrm{sim},i})^2}{\sum_{i=1}^{n}(Q_{\mathrm{obs},i} - \bar{Q}_{\mathrm{obs}})^2} \tag{7}$$

where: Q_{obs}= observed values, Q_{sim}= predicted) values and $\bar{Q}_{\mathrm{obs}}$= mean of the observed values. In hydraulic modeling, the Nash–Sutcliffe Efficiency (NSE) has a theoretical range from −∞ to 1, where a value of 1 denotes perfect agreement between observed and predicted data. Generally, an NSE value greater than 0.50 indicates satisfactory model performance, while values above 0.75 are considered to represent very good predictive accuracy **(Moriasi et al., 2007).** Dimensional analysis is a strong tool to perceive the correlations between physical parameters in fluid dynamics. The method is used in the investigation of hydraulic jumps in horizontal prismatic channels.

The present investigation was conducted as an experimental laboratory study rather than a physical scale model of a specific hydraulic structure. Accordingly, no prototype was considered in this work, and geometric or dynamic similarity between a model and a prototype was not established. The dimensional analysis was performed solely to identify the governing dimensionless parameters influencing hydraulic jump characteristics. The available laboratory facilities, including the flume, pump, and associated equipment determined the dimensions of the experimental setup.
According to hydraulic jump theory, the main variables affecting the jump pattern and energy loss are: (a) fluid properties including fluid mass density (ρ), kinematic viscosity (μ), and gravitational acceleration (g), (b) experimental channel properties including width, sill height, the position of the sill and channel bed roughness (B, hs, Ls and ε), (c) Important inflow features include the flow depths before and after the jump (y_1, y_2) and the velocities on both sides of the jump (V_1, V_2). These can be explored as:

$$f(y_1, y_2, h_s, V_1, V_2, L_s, \rho, g, \mu, \varepsilon) = 0 \tag{8}$$

- All experiments were conducted in a flume with glass sidewalls and a stainless-steel bed. For a hydraulically smooth channel bed, the effect of bed roughness (ε) is considered negligible.
- Applying the continuity equation leads to a simplified relationship, expressed as follows:

$$q = V_1 y_1 = V_2 y_2 \tag{9}$$

$$V_2 = \frac{V_1 y_1}{y_2} \tag{10}$$

- Reducing the characteristic parameters further simplifies Eq. (7) as follows:

$$f(y_1, y_2, h_s, V_1, L_s, \rho, g, \mu) = 0 \tag{11}$$

- The sill position (Ls) cannot be determined analytically; the function f must therefore be defined experimentally.

Buckingham's π theorem generates dimensionless governing groups for the phenomenon, with the number of π terms defined as:

$$K = n - m \tag{12}$$

Where: K is the number of dimensionless groups (π terms), n is the number of variables (8) and m is the number of fundamental dimensions (3). Thus, K = 5
The set of repeating variables was choosing that include all the fundamental dimensions. A common choice for the repeating variables in fluid dynamics involving open channel flow are y_1, V_1, and ρ. Using these repeating variables to form dimensionless groups with the other variables.

1. Dimensionless group for downstream flow depth, π_1:

$$\pi_1 = y_2 / y_1 \tag{13}$$

2. Dimensionless group for sill hight, π_2:

$$\pi_2 = h_s / y_1 \tag{14}$$

3. Dimensionless group for sill position, π_3:

$$\pi_3 = L_s/y_1 \quad (15)$$

By dividing π_3 by π_2, the resulting expression reduces to the geometric ratio L_s/h_s, which is particularly advantageous for engineering design and applied analysis

$$\pi_4 = L_s/h_s \quad (16)$$

4. Dimensionless group for flow velocity ratio (Froude Number), π_4:

$$\pi_5 = V_1/\sqrt{gy_1} \quad (17)$$

5. Dimensionless group for viscosity (Reynolds Number), π_5:

$$\pi_6 = \rho V_1 y_1/\mu \quad (18)$$

$$\pi_1.\pi_4.\pi_5.\pi_6 = \left(\frac{y_2}{y_1}, \frac{L_s}{h_s}, Fr_1, R_e\right)$$

$$\frac{L_s}{h_s} = \left(\frac{y_2}{y_1}, Fr_1, R_e\right) \quad (19)$$

The experimental data were analyzed using SPSS (Version 25.0). Following the dimensional analysis, the governing dimensionless parameters were selected as the independent variables, while the hydraulic jump characteristics were treated as the dependent variables. Nonlinear regression analysis was then performed using the curve-fitting procedure available in SPSS to develop empirical equations describing the relationships between these variables. The developed equations were evaluated using the coefficient of determination (R^2) and the Nash–Sutcliffe Efficiency (NSE), and the equations with the highest goodness-of-fit and physically meaningful behavior were selected for further analysis.

3. RESULTS AND DISCUSSION

Experiments were carried out on an open horizontal channel provided with a discharge gate at the upstream end and a thin sill at the base to generate hydraulic jumps. The study aimed to assess the impact of sill heights and locations on basic hydraulic jump characteristics such as the sequential depth ratio, jump length, and free surface profile in a stilling basin. Different sill heights and locations in relation to the starting point of the hydraulic jump (toe) were tested downstream of the sluice gate. Several experiments were carried out based on initial Froude numbers. Experimental data indicated that the sill did not affect the sequent depth ratio much. Nonetheless, a movable sill was used since it proved to be effective in decreasing hydraulic jump length. Moreover, the sill improves the jump's stability and prevents it from being thrown out of the basin. The uncertainty analysis indicated that the propagated uncertainties of the calculated hydraulic parameters were small relative to the measured values, confirming the reliability of the experimental data **(Taylor, 1997).**

Fig. 3 graphically shows the relationship between y_2/y_1 and Fr_1 indicates that the subsequent depth ratio, y_2/y_1, rises as the initial Froude number increases. The figure also demonstrates that the trend between y_2/y_1 and Fr_1 follows a linear pattern. Moreover, the experimentally recorded data were compared to Belanger's equation for assessing the efficiency of sills in dissipating energy and verify the accuracy of the recorded data.

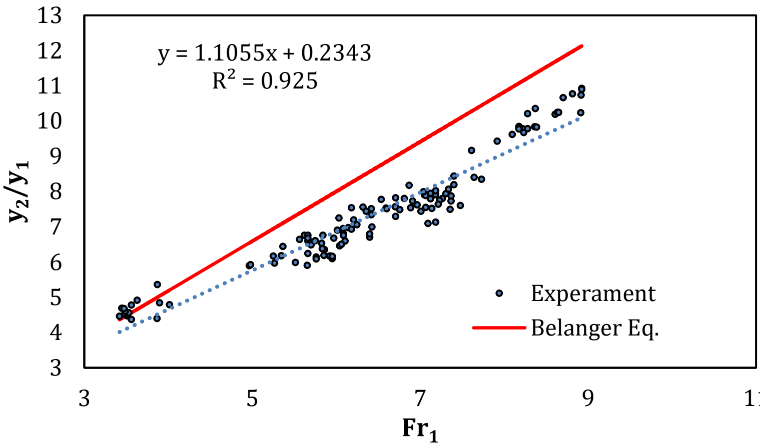

Figure 3. The relationship between y_2/y_1 and Fr_1.

On the other hand, the Nash–Sutcliffe Efficiency (NSE) was employed to evaluate the agreement between the observed and predicted data. The computed NSE value for the observed and predicted (y_2/y_1) ratio was 0.73, indicating good model performance and demonstrating a satisfactory level of agreement between the observed and predicted data. Belanger's equation establishes the relationship between upstream depth and downstream depth in a hydraulic jump, using the Froude number to quantify gravity's effect on flow **(Chaudhry, 2008)**. It is essential in hydraulic engineering for energy dissipation and channel design.

$$\frac{y_2}{y_1} = \frac{1}{2} * \left(\sqrt{1 + 8 * Fr_1^2} - 1\right) \quad (20)$$

Fig. 3 shows that the experimental y_2/y_1 values are lower than the theoretical y_2/y_1 values due to the effect of the thin sill placed at the bottom of the channel.
From the curve fitting, the following equation was derived to estimate y_2/y_1 values corresponding to a given Fr_1 with the determination coefficient of (R^2 = 0.925):

$$\frac{y_2}{y_1} = 1.055Fr_1 + 0.234 \quad (21)$$

A straightforward polynomial regression applied to all the analysed data revealed a formula for calculating the hydraulic jump sequent depth ratio with the determination coefficient of (R^2 = 0.96):

$$\frac{y_2}{y_1} = 0.1162Fr_1^2 - 0.3217Fr_1 + 4.3778 \quad (22)$$

As demonstrated in **Fig. 3**, the functional relationships derived from Belanger's equation indicate that the upstream depth ratio (y_2/y_1) tends to increase with higher sill height ratios (h_s/L_s) and greater Froude numbers. More specifically, for a given initial Froude number, as the sill height increases, the value of h_s/L_s also increases, and consequently, the subsequent depth (y_2) increases. This trend highlights the significant influence of the sill height (hs) on the energy exchange and dissipation processes, with the length of the basin (Ls) remaining constant. The increase in the sequent depth ratio with increasing initial Froude number is attributed to the higher momentum and kinetic energy of the approaching supercritical flow. Raising the sill height increases the downstream water level and the sequent depth ratio, which are necessary to maintain momentum balance. This intense momentum exchange simultaneously enhances turbulence and energy dissipation within the hydraulic jump. A higher sill raises the downstream water level, increasing the pressure required to satisfy momentum conservation.

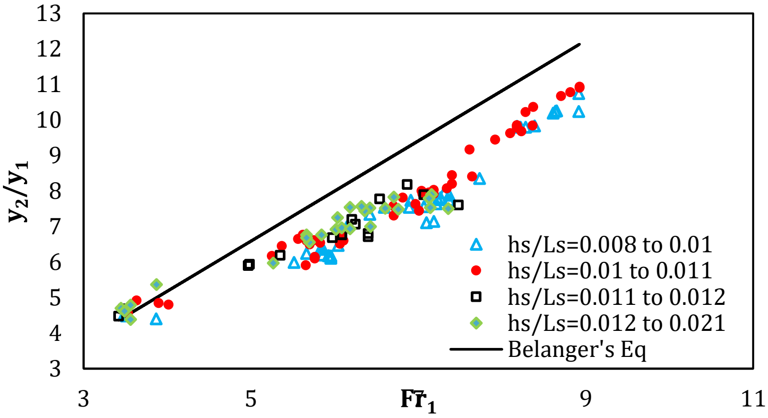

Figure 4. The variation of y_2/y_1 with Fr_1 for various hs/Ls, when the Ls is constant.

Further studies were conducted to determine the relationship between hydraulic jump length and the initial Froude number (Fr_1). **Fig. 5** depicts the fitted correlations for the hydraulic jump length ratio (L_j/y_1) vs Fr_1. Also shows that Froude's number has a linear relationship with L_j / y_1

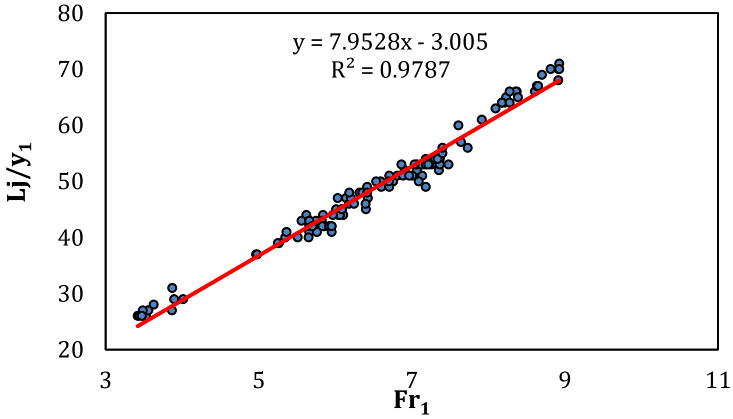

Figure 5. The hydraulic jump length ratio (L_j/y_1) versus Fr_1.

The equation below expresses a linear relationship between Fr_1 and Lj/y_1 with determination coefficient of (R^2 = 0.98):

$$\frac{L_j}{y_1} = 7.95Fr_1 - 3 \tag{23}$$

The increased downstream water depth produced by the movable sill provides the tailwater conditions required for hydraulic jump formation at an earlier location. Consequently, the momentum balance is achieved over a shorter distance, causing the flow to transition from supercritical to subcritical conditions closer to the sluice gate. This shortens the hydraulic jump and improves its stability within the stilling basin.

Fig. 6 demonstrates an inverse relationship between the distance of the thin sill from the jump toe and its effect on jump length: greater distance means less effect. Furthermore, at a given distance, a higher sill produces a proportionally greater reduction in the length of the hydraulic jump. Hydraulically, as the Froude number increases mean the incoming flow possesses greater inertial forces and kinetic energy relative to gravity, which necessitates a longer, more turbulence to decelerate the water and dissipate the excess energy.

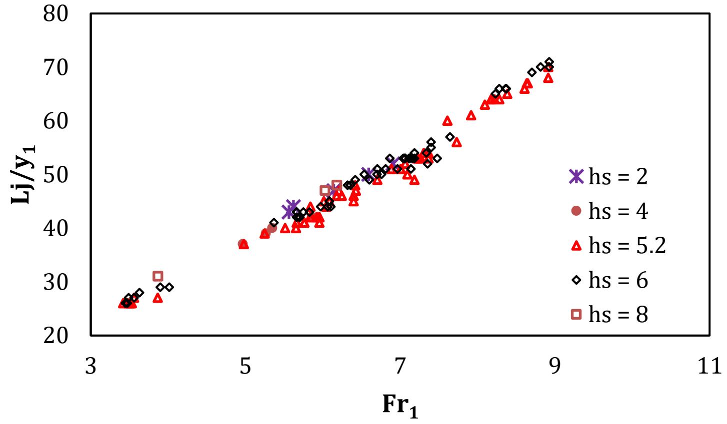

Figure 6. The L_j/y_1 versus Fr_1, for various hs/Ls, when the Ls is constant

Fig. 7 graphically presents the relationship between the upstream Froude number and the hydraulic jump length ratio. Additionally, the following equation provides a method for calculating L_j/y_2 based on a known Fr_1 with determination coefficient of (R^2 = 0.82):

$$\frac{L_j}{y_2} = -0.075Fr_1^2 + 1.089Fr_1 + 2.78 \quad (24)$$

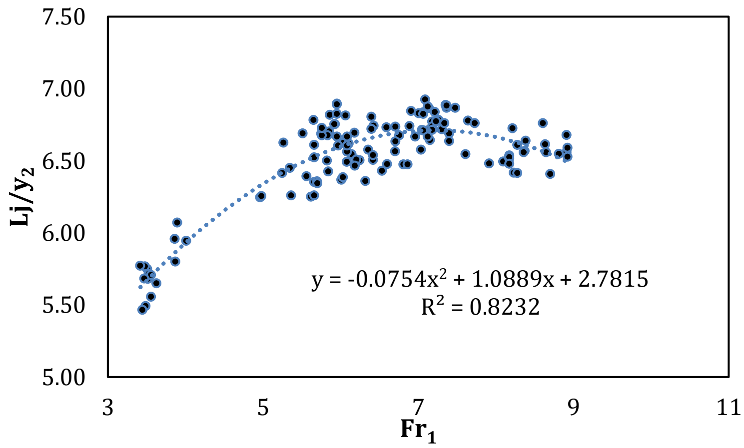

Figure 7. The L_j/y_2 with the Fr_1.

To observe the friction effects on the downstream height of the jump during control by a thin sill, the experimental sequent depth (y_{2exp}) was compared with the theoretical sequent depth (y_{2Theo}) as calculated using Belanger's equation, as shown in **Fig. 8**. The results show that the values of y_{2exp} were consistently lower than the values of y_{2Theo} due to the fixation of the thin sill at the downstream of the hydraulic jump. This confirmed that friction had a noticeable effect on the final relative depth of the hydraulic jump **(Hager and Bretz, 1986)**. As illustrated in **Fig. 9**, the observed values of y_2/y_1 exhibited close agreement with values computed using Belanger's equation, with deviations not exceeding 5%.

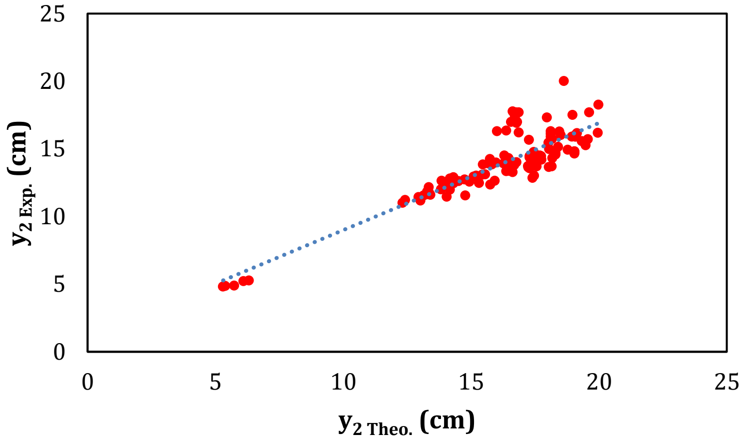

Figure 8. Comparison between (y_{2Exp}) with (y_{2Theo}), as determined using Belanger's equation.

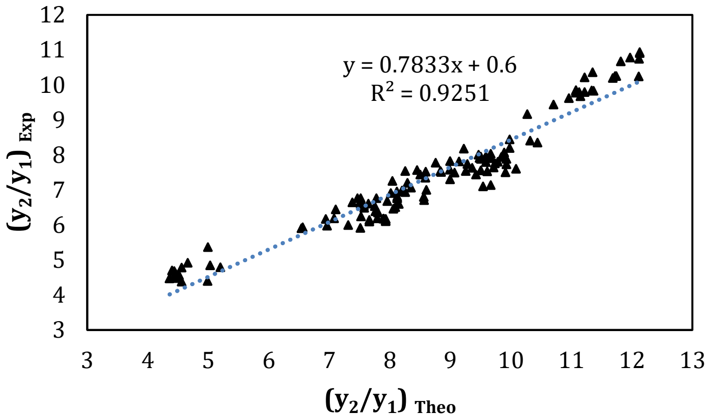

Figure 9. The observed values of y_2/y_1 via values computed using Belanger's equation.

In open channels, the measured energy loss (ΔE) during a hydraulic jump is determined as the difference between upstream and downstream energies ($E_1 - E_2$). The energy at each section is calculated using the relation **(Chaudhry, 2008)**:

$$E_i = y_i + \frac{v_i^2}{2g} \tag{25}$$

As shown in **Fig. 10**, relative energy loss ($\Delta E/E_1$) increases nonlinearly with the initial Froude number (Fr_1). This strong correlation (R^2 = 0.98) is modelled by the following regression-based equation:

$$\left(\frac{\Delta E}{E_1}\right)_{exp} = 0.017Fr_1^2 + 0.28Fr_1 - 0.45 \tag{26}$$

The increased downstream depth created by the movable sill strengthens turbulence and recirculation within the hydraulic jump, enhancing the mixing between the supercritical and subcritical flows. This converts a larger portion of the flow's kinetic energy into turbulent energy, resulting in greater energy dissipation within the stilling basin.

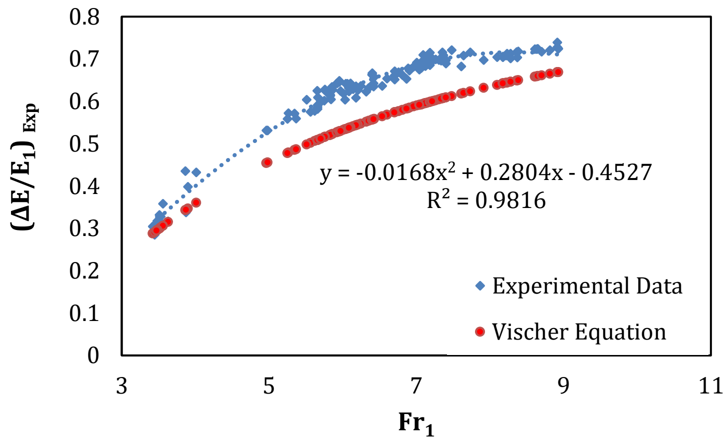

Figure 10. Experimental relative energy loss with Fr_1.

The following equation by Vischer and Hager is also plotted for comparison **(Vischer and Hager, 1996)**.

$$\frac{\Delta E}{E_1} = \frac{1}{8}\frac{\left(\sqrt{1+8*Fr_1^2}-3\right)^3}{(2+Fr_1^2)\left(\sqrt{1+8*Fr_1^2}-1\right)} \tag{27}$$

Fig. 10 shows a good agreement between Vischer and Hager's equation results and the experimental data of this study with a determination coefficient of (R^2=98).

The efficiency of a hydraulic jump is expressed by the dimensionless ratio E_2/E_1, which represents the amount of initial energy retained after the jump. The energy efficiency equation, presented below, demonstrates its severe dependency on the upstream Froude number **(Yager, 1960)**

$$\frac{E_2}{E_1} = \frac{E_1-\Delta E}{E_1} = \frac{(8Fr_1^2+1)^{3/2}-4Fr_1^2+1}{8Fr_1^2(2+Fr_1^2)} \tag{28}$$

Fig. 11 presents the energy dissipation efficiency of the hydraulic jump model Eq. (21) relative to the experimental jump versus Fr_1. Results indicate the model's average relative energy loss exceeded the experimental value by 4.87%

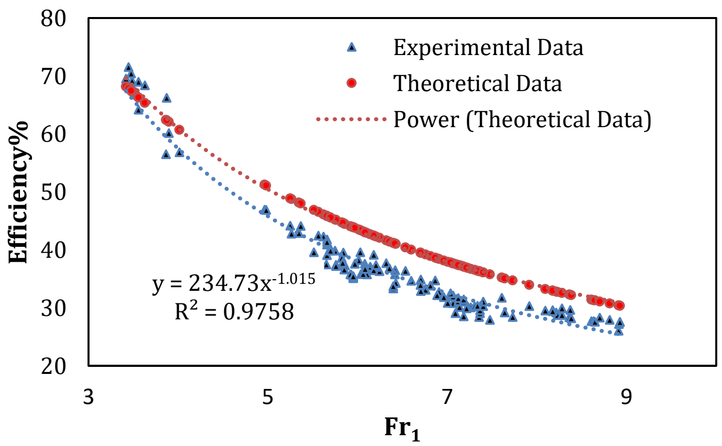

Figure 11. The energy dissipation efficiency, relative to the experimental jump versus Fr_1.

Research trends often use experimental results to calculate end sill location and height using regression. However, linear regression fails to fit the equation for sill location based on independent variables. Using (SPSS v. 25) software, a nonlinear regression using a power multiplicative function was tried, with a determination coefficient of 0.92, resulting in an acceptable expression for sill location per initial depth of the jump.

$$\frac{L_s}{y_1} = 25.187 + \left(\frac{y_2}{y_1}\right)^{2.586} + \left(\frac{h_s}{y_1}\right)^{0.367} + \left(\frac{\log Re}{Fr_1^{0.477}}\right)^{3.166} \quad (29)$$

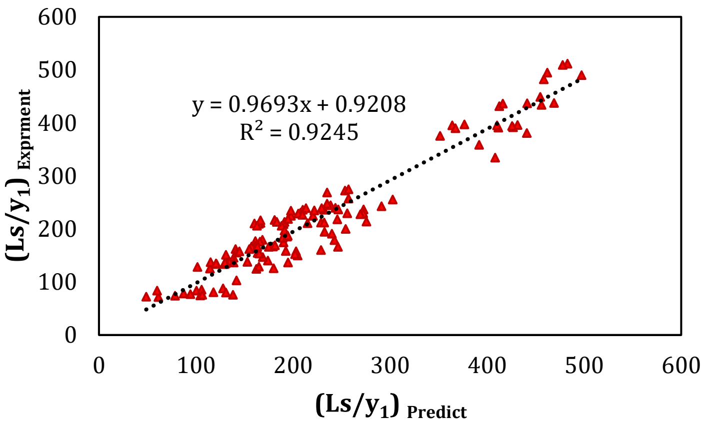

Figure 12. The experiment and predicted data of the sill location per initial jump depth.

As illustrated in **Fig. 12**, the sill location per initial depth of the jump was estimated using this equation and plotted against the observed one. This figure demonstrates the good agreement between the experiment and predicted data. The sill regulates the downstream water level by increasing the local flow depth upstream of the sill, thereby creating the tailwater conditions required for hydraulic jump formation. Adjusting the sill height and location controls the downstream water level and helps stabilize the hydraulic jump within the stilling basin.

Fig. 13 depicts that the revealed sill location-to-height ratio (Ls/hs) was significantly correlated with the initial Froude number, Reynolds number, and sequent depth ratio, achieving a determination coefficient (R^2) of 0.89.

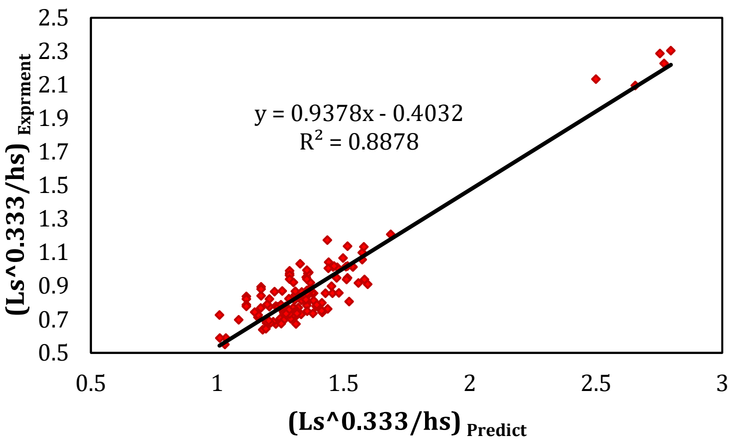

Figure 13. Comparison between the experimental results and the prediction of the sill location to height ratio with the initial Froude number.

This confirms a strong relationship captured by the regression model.

$$\frac{\sqrt[3]{L_s}}{h_s} = 10.96 - 0.1\left(\frac{y_2}{y_1}\right) + 0.01Fr_1 - 2(\log R_e) \quad (30)$$

The close agreement between the experimental and predicted values is supported by the reported coefficients of determination (R^2=0.82-0.98), indicating that the developed regression models adequately represent the experimental data within the investigated range.

4. CONCLUSIONS

This study presented new experimental findings on the application of a thin-crested sill for controlling hydraulic jumps in rectangular channels. Based on the results, the following conclusions were drawn:

1. The ratios of the experimental sequent depths (y_2/y_1) were consistently lower than the predictions of Belanger's equation, which confirms the efficiency of the sill in energy dissipation and validating the data.
2. The sequent depth ratio (y_2/y_1) increases with the initial Froude number (Fr_1).
3. The ratio of hydraulic jump length (L_j/y_1) is linearly proportional to Fr_1, while L_j/y_2 does not. The value of L_j/y_1 is useful in estimating the jump lengths.
4. The experimental sequent depths (y_{2exp}) were consistently lower than the theoretical predictions due to the fixed thin sill downstream of the hydraulic jump, indicating that friction significantly affected the final relative depth.
5. The relative energy loss ($\Delta E/E_1$) increases with increasing Fr_1. A regression equation developed for this energy loss showed good agreement with the equation proposed by Vischer and Hager.
6. The theoretical model of hydraulic jump had an average overestimation of 4.87% of the actual dissipation efficiency with the experimental results.
7. The nonlinear regressions models are used to predict the hydraulic jump parameters and sill positioning, and it is confirmed that sill height and the location have a great impact on the behaviour of the jump.

Acknowledgements

The authors gratefully acknowledge the Hydraulics laboratory staff in the Department of Water Resources Engineering within the College of Engineering at the University of Sulaimani. Without their help and contribution, this work would not have been accomplished.

Credit Authorship Contribution Statement

Rizgar A. Karim: Writing Original draft, investigation, methodology, data formatting and results analysis. Bahram A. Faraj: Writing - Review and editing, model design and fabrication, and laboratory Works.

Declaration of Competing Interest

The authors declare that they have no known competing financial interests or personal relationships that could have appeared to influence the work reported in this paper.

REFERENCES

Abbaszadeh, H., Daneshfaraz, R., and Norouz, R., 2023. Experimental investigation of hydraulic jump parameters in sill application mode with various syntheses. *Journal of Hydraulic Structures*, 9(1), pp. 18–42. https://doi.org/10.22055/jhs.2023.43208.1245

Achour, B., and Amara, L., 2023. Control of the hydraulic jump by a broad-crested sill in a rectangular channel: New theory and experiment. *Larhyss Journal*, 20(2), pp. 111–140.

Achour, B., and Debabeche, M., 2003. Control of hydraulic jump by sill in a U-shaped channel. *Journal of Hydraulic Research*, 41(1), pp. 97–103.

Akan, A.O., and Iyer, S.S., 2021. *Open Channel Hydraulics*. Butterworth-Heinemann.

Al-Suhili, R.H.S., Karim, R.A., and Qadir, W.E., 2023. Discharge coefficient of contracted rectangular sharp-crested weirs: An experimental study. *Journal of Engineering*, 29(6), pp. 1–16. https://doi.org/10.31026/j.eng.2023.06.01

Alikhani, A., Behrozi-Rad, R., and Fathi-Moghadam, M., 2010. Hydraulic jump in stilling basin with vertical end sill. *International Journal of Physical Sciences*, 5(1), pp. 25–29. https://doi.org/10.5897/IJPS.9000293

Bachir, A., Amara, L., and Mehta, D., 2022. Control of the hydraulic jump by a thin-crested sill in a rectangular channel: New experimental considerations. *Larhyss Journal*, 19(2), pp. 141–157.

Chaudhry, M.H., 2008. *Open-Channel Flow*. Second Edition, Springer. New York https://doi.org/10.1007/978-0-387-68648-6

Chow, V.T., 1959. *Open-Channel Hydraulics*. McGraw-Hill, New York.

Daneshfaraz, R., Morouzi, R., Ebadzadeh, P., Di Francesco, S., and Abraham, J.P., 2023. Experimental study of geometric shape and size of sill effects on the hydraulic performance of sluice gates. *MDPI. Water*, 15(2), pp. 1-16. https://doi.org/10.3390/w15020314

Dardeer, M.A., 2022. Studying the effect of triangular sill on hydraulic jump. *Civil Engineering Research Magazine*, 44, pp. 216–234.

Debabeche, M., and Achour, B., 2007. Effect of sill on hydraulic jump in a triangular channel. *Journal of Hydraulic Research*, 45(1), pp. 135–139. https://doi.org/10.1080/00221686.2007.9521753

Dixit, P., Shet, R., Kansagara, K., Wanjari, P., Jadhav, S., and Karkhanis, A., 2016. Control of hydraulic jump using abrupt rise inbed. *International Journal of Modern Trends in Engineering and Research*. 3(4).

Eltoukhy, M.A.R., 2016. Hydraulic jump characteristics for different open channel and stilling basin layouts. *International Journal of Civil Engineering and Technology*, 7(2), pp. 290–301.

Erryanto, S., and Dermawan, V., 2024. Double sill stilling basin to enhance energy dissipation. IOP Conference Series: *Earth and Environmental Science*. https://doi.org/10.1088/1755-1315/1311/1/012009

Fathi-Moghadam, M., Haghighipour, S., Lashkar, B., and Aghtouman, P., 2011. Reduction of stilling basin length with tall end sill. *Journal of Hydrodynamics*, 23(4), pp. 498–502. https://doi.org/10.1016/S1001-6058(10)60141-2

Forster, J.W., and Skrinde, R.A., 1950. Control of the hydraulic jump by sills. *Transactions of the ASCE*, 115(1), pp. 973–987. https://doi.org/10.1061/TACEAT.000634

Ghordnooshahre, A., Omid, M.H., Kooshakzadeh, S., 2010. The effect of broad-crested sill on the hydraulic jump characteristics in diverging stilling basins. *Iranisn Journal of soil and Water Research*. 41(1), Number 256745. https://dor.isc.ac/dor/20.1001.1.2008479.1389.41.1.8.7

Gupta, S.K., and Mehta, R.C., 2010. Modeling of hydraulic jump characteristics in horizontal prismatic channels. In: *Proceedings of MSHTFF Conference*.

Hager, W.H., 2013. Energy Dissipators and Hydraulic Jump. *Springer*. https://doi.org/10.1007/978-94-015-8048-9

Hager, W.H., and Bretz, N.V., 1986. Hydraulic jumps on rough beds. *Journal of Hydraulic Research*, 24(5), 307–314.

Hager, W.H., and Li, D., 1992. Sill-controlled energy dissipator. *Journal of Hydraulic Research*, 30(2), pp. 165–181. https://doi.org/10.1080/00221689209498932

Jadhav, S., and Karkhanis, A., 2016. Control of hydraulic jump using abrupt rise in bed. *International Journal of Sciences Technology and Management*, 6(4), pp. 22–29.

Jamshidi, A., Bejestan, M.S., Rahmanshahi, M., and Bahrami-Yarahmadi, M., 2025. Impact of continuous and dentate transverse baffles on vertical drop structure basin dimensions. *Iranian Journal of Science and Technology, Transactions of Civil Engineering*. https://doi.org/10.1007/s40996-025-02058-z.

Karim, R.A., and Mohammed, J.R., 2020. CFD and PIV comparison for velocity distribution over spillways. *Heliyon*, 6(10), pp. 1–9. https://doi.org/10.1016/j.heliyon.2020.e05165

Kim, Y., Choi, G., Park, H., and Byeon, S., 2015. Hydraulic jump and energy dissipation with sluice gate. *Water*, 7(9), pp. 5115–5133. https://doi.org/10.3390/w7095115

Li, C.F., 1995. Determining the location of hydraulic jump by model test. *Ohio University*.

Mahmoud, S.H., and Mohamed, R.F., 2022. Effect of unconventional sills on energy dissipation. *Journal of Al-Azhar University Engineering Sector*, 17(65), pp. 1157–1172. https://doi.org/10.21608/auej.2022.265706

Moriasi, D., Arnold, J., Liew, M.W., and Veith, T. L., 2007. Model evaluation guidelines for systematic quantification of accuracy in watershed simulations. *Journal of ASABE*. 50(3). https://doi:10.13031/2013.23153

Movahed, S.A.M., Mozaffari, J., Davoodmaghami, D., and Akbari, M., 2018. Semi-analytical equation to estimate hydraulic jump length. *Periodica Polytechnica Civil Engineering*, 62(4), pp. 1001–1006. https://doi.org/10.3311/PPci.11257

Mundo-Molina, M., and Díaz Pérez, J.L., 2019. Estimation of hydraulic jump length in rectangular channel. *Journal of Water Resource and Protection*, 11(12), pp. 1481–1488. https://doi.org/10.4236/jwarp.2019.1112086

Nandi, B., Das, S., and Mazumdar, A., 2020. Experimental and numerical simulation of hydraulic jump. *IOP Conference Series: Earth and Environmental Science*. https://doi.org/10.1088/1755-1315/505/1/012024

Omid, M.H., Kouchakzadeh, S., and Gord-Noshahri, A., 2010. Sill-controlled hydraulic jump in expanding channel. *Proceedings of ICE – Water Management*, 163(10), pp. 515–522. https://doi.org/10.1680/wama.900085

Pagliara, S., and Peruginelli, A., 2000. Adverse-slope hydraulic jump control. *Journal of Hydraulic Engineering*, 126(11), pp. 847–851. https://doi.org/10.1061/(ASCE)0733-9429(2000)126:11(847)

Samadi-Boroujeni, H., Ghazali, M., Gorbani, B., and Nafchi, R. F., 2013. Effect of triangular corrugated beds on hydraulic jump characteristics. *Canadian Journal of Civil Engineering*, 40(9), pp. 841–847. https://doi.org/10.1139/cjce-2012-0019

Taylor, J.R., 1997. *An introduction to error analysis - the study of uncertainties in physical measurements*. University Science Books. University of Colorado

Vischer, D., and Hager, W.H., 1996. *Energy Dissipators*. University of California.

Yager, W.C., 1960. *Open channel hydraulics* (review of Chow, V.T.). McGraw-Hill.

Yıldız, A., Marti, A. I., Yarar, A., and Yilmaz, V., 2020. Determination of hydraulic jump position using CFD. *Romanian Journal of Ecology Environmental Chemistry*, 2(2), pp. 78–85. https://doi.org/10.21698/rjeec.2020.211

دراسة تجريبية للتحكم في القفزة الهيدروليكية في القنوات المستطيلة باستخدام عتبات متحركة رقيقة القمة

رزكار أحمد كريم*، بهرام عبد الرحمن فرج

قسم هندسة الموارد المائية، كلية الهندسة, جامعة السليمانية, السليمانية, العراق

الخلاصة

تُعدّ القفزات الهيدروليكية ظاهرة أساسية في هيدروليكا القنوات المفتوحة، وتلعب دورًا حاسمًا في تبديد الطاقة وتصميم أحواض التسكين. أُجري بحث تجريبي لدراسة القفزة الهيدروليكية المُتحكَّم بها باستخدام عتبة رقيقة القمة ذات ارتفاعات ومواقع مُختلفة، وهو موضوع لم يُدرس سابقًا. لذلك، أُجريت هذه الدراسة التجريبية للتحقق من التحكم في القفزة الهيدروليكية باستخدام عتبة رقيقة القمة ذات ارتفاعات ومواقع مُختلفة. من الضروري معرفة الموقع الدقيق للقفزة الهيدروليكية داخل القناة المفتوحة الأفقية لتجنب أي ضرر قد يلحق بالمنشآت المُحيطة. في المجمل، أُجريت 130 تجربة بأرقام فرود ابتدائية تتراوح من 3.42 إلى 8.93. شملت القياسات المتغيرات الأساسية، مثل الأعماق الابتدائية والمتتابعة، وأطوال القفزات، وفقدان الطاقة لفتحات بوابات السد، ومعدلات التصريف المختلفة. تُشير النتائج إلى أنه على الرغم من أن موضع العتبة كان له تأثير ضئيل على نسبة العمق المتتابع، إلا أنه أدى إلى انخفاض كبير في طول القفزة وموقعها وتبديد الطاقة في حوض التهدئة. أظهرت نسبة العمق المتتابع التجريبية (y_2/y_1) توافقًا وثيقًا مع القيم المتوقعة من معادلة بيلانجر. بالإضافة إلى ذلك، حققت نماذج الانحدار المُطوَّرة لتقدير نسبة العمق المتتابع، وطول القفزة، وفقدان الطاقة، والموقع الأمثل للعتبة، معاملات تحديد تتراوح بين 0.82 و0.98. تُقدِّم هذه النتائج إرشادات تصميم عملية لاختيار أبعاد ومواقع العتبة المناسبة لضمان تكوين القفزة الهيدروليكية بشكل كامل وتبديد الطاقة بكفاءة في أحواض التسكين.

الكلمات المفتاحية: عتبة متحركة رقيقة القمة، التحكم في القفزة الهيدروليكية، ارتفاع العتبة، موضع العتبة، حوض التسكين.